Theoretical Study of α/*β*-Alanine and Their Protonated/Alkali Metal Cationized Complexes

S. Abirami,[†,‡] Y. M. Xing,[§] C. W. Tsang,*[,§] and N. L. Ma*[,†]

Institute of High Performance Computing, 1 Science Park Road, #01-01, The Capricorn, Singapore Science Park II, Singapore 117528, National Institute of Education, Science and Technology Education, 1 Nanyang Walk, Singapore 637616, and Department of Applied Biology and Chemical Technology, The Hong Kong Polytechnic University, Hung Hom, Hong Kong

Received: June 16, 2004; In Final Form: October 20, 2004

Density functional theory has been employed to model the structure and the relative stabilities of α/*β*-alanine conformers and their protonated and alkali metal cationized complexes. In general, we find that the behavior of the *β*-alanine (*β*-Ala) system is quite similar to that of α-alanine (α-Ala). However, the presence of the methylene group (−CH_2−) at the *β* position in *β*-Ala leads to a few key differences. First, the intramolecular hydrogen bonding patterns are different between free α- and *β*-Ala. Second, the stability of zwitterionic species (in either the free ligand or alkali metal cationized complexes) is often enhanced in *β*-Ala. Third, the preferred mode of alkali metal cation (M^+) binding may also differ in α- and *β*-Ala. Natural energy decomposition analysis has been applied here to gain further insight into the effects of the ligand, cation size, and mode of binding on the nature of interaction in these M^+−Ala complexes.

Introduction

Although less abundant than the corresponding α-amino acids, *β*-amino acids (and its derivatives) can be found in nature.[1] The *β*-amino acid taurine (2-aminoethane sulfonic acid) has been suggested to be involved in the regulation of transcription processes.[2] Among bioactive peptides containing *β*-amino acids (*β*-peptides), *β*-alanine (Scheme 1) is most commonly found.[1] For example, (*β*-alanine)-tyrosine (a paralysin) is a toxin playing active roles in the metamorphosis of insects.[3] Possibly because of its higher metal chelation and free-radical scavenging abilities, (*β*-alanine)-histidine (carnosine) has been used as an anti-aging supplement,[4] and more recently, has shown to be able to prevent ischemic acute renal failure in rats.[5] Moreover, peptides containing *β*-amino acids are more resistant to protease degradations than their α-amino acid analogues.[6] Because of these reasons, *β*-peptides are recognized to be a potentially important class of biomedical and therapeutic compounds.[7]

Protonation is a common and important process in biological systems. Alkali metal cations (M^+) like Na^+ and K^+ are among the most abundant metal cations found in biological systems,[8] playing important roles in many fundamental biological processes and enzyme functions. Studies on H^+/M^+ binding affinities (or energies, i.e., enthalpies of binding, ΔH) to small model *β*-amino acids/peptides form the basis of the detailed understanding of these interactions in the more complex and larger biological systems. Studies in the gas phase have the distinct advantage of determining the intrinsic properties of molecules, without the complicating effects of the solvent. While the intrinsic proton and alkali metal binding affinities in the gas phase have become available for α-amino acids/peptides in recent years,[9,10] related information is very limited for the corresponding *β*-amino acids/peptides, and only very recently, the gas-phase proton affinity (PA) of *β*-Ala has been determined.[11] In this work, we carried out systematic theoretical study on free α- and *β*-Ala and their protonated and alkali metal cationized (M^+, where $M^+ = Li^+$, Na^+, and K^+) complexes to understand the similarity/difference of these two amino acids.

SCHEME 1

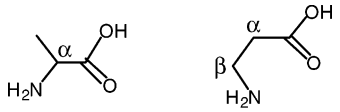

α-Ala β-Ala

Materials and Methods

The initial geometries of various α-Ala species were obtained from literature[12−14] and fully reoptimized at the same level of theory as the *β*-Ala systems (see details next). As the *β*-Ala systems is less well-studied theoretically, initial trial structures of Li^+-*β*-Ala were obtained using the SYBYL package,[15] one in the charge solvated and one in the zwitterionic form. Other charge solvated and zwitterionic isomers were generated via the random search technique, with the minimization step carried out using the MMFF94s force field. All these species were then reoptimized at the HF/6-31G(d) level, using the GAUSSIAN98 package of programs[16] on IBM p690. On the basis of the stability of different conformers calculated at this level, the two most stable charge solvated (with different binding modes) and zwitterionic complexes were retained for further geometry refinement. The corresponding Na^+ and K^+ complexes were obtained by replacing the Li^+ with Na^+ and K^+, respectively, followed by full geometry optimization.

During the exploratory phase of our study, we found that the geometries of some M^+-*β*-Ala complexes are very sensitive to the level of theory employed, both in terms of the electron correlation method used and the choice of basis sets. As an

* Corresponding authors. E-mail: (C.W.T.) bcctsang@polyu.edu.hk; (N.L.M.) ida@ihpc.a-star.edu.sg.
† Institute of High Performance Computing.
‡ National Institute of Education.
§ Hong Kong Polytechnic University.

10.1021/jp047399o CCC: $30.25
Published on Web 12/29/2004

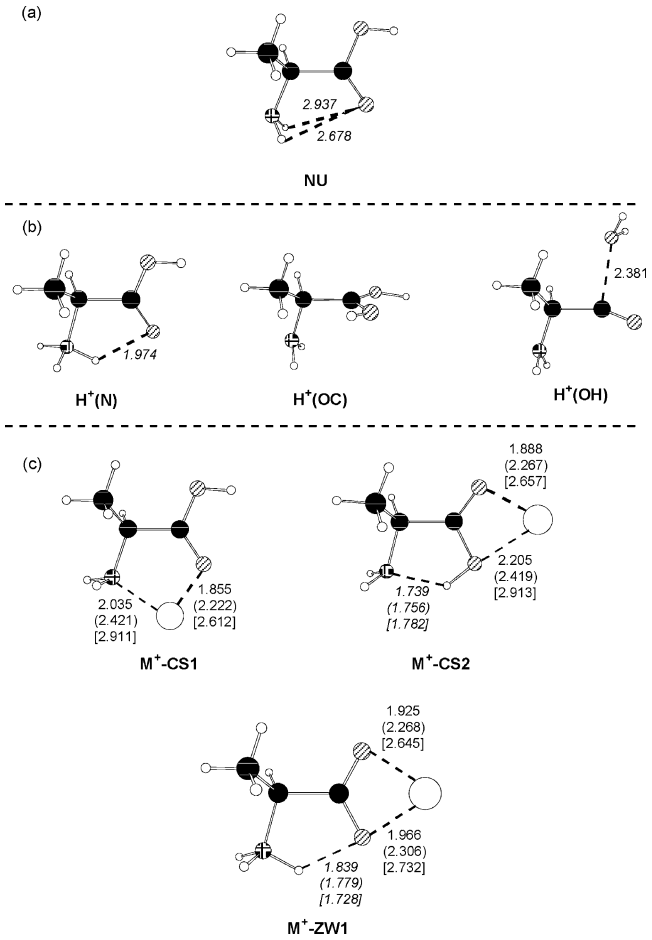

Figure 1. Optimized geometries (at B3LYP/6-31+G(d) level) for (a) α-Ala, (b) protonated α-Ala, and (c) alkali metal cationized α-Ala, with the geometrical parameters (in unit of Å) of M^+-α-Ala for $M^+ = Li^+$, Na^+, and K^+ given in normal font, parentheses, and square brackets, respectively. The distance of intramolecular hydrogen bond (in unit of Å) is given in italics.

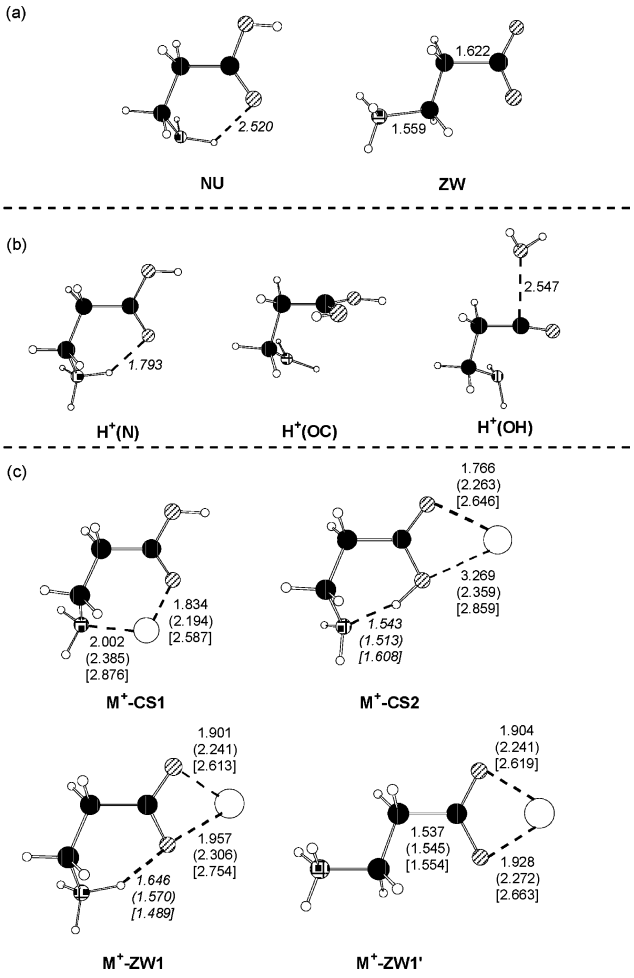

Figure 2. Optimized geometries (at B3LYP/6-31+G(d) level) for (a) β-Ala, (b) protonated β-Ala, and (c) alkali metal cationized β-Ala, with the geometrical parameters (in unit of Å) of M^+-β-Ala for $M^+ = Li^+$, Na^+, and K^+ given in normal font, parentheses, and square brackets, respectively. The distance of intramolecular hydrogen bond (in unit of Å) is given in italics.

example, one of the K^+-β-Ala zwitterionic complexes (denoted as **K^+−ZW1** next) is rather elusive. At many levels of theories, sensible starting structures collapsed to the charge-solvated form (denoted as **K^+−CS2** next). Using MP2(full)/6-311+G(3df,2p) as the benchmark, the existence of the **K^+−ZW1** complex was confirmed. Problems were also found in the **Li^+−ZW1**/**Li^+−CS2** pair, in which geometry optimization at various levels tends to yield **Li^+−ZW1** but not **Li^+−CS2**. All these suggested that the proton shift between -OH and -NH_2 sites for the various M^+-β-Ala complexes is rather facile when compared to the α-Ala systems. After careful consideration, the B3-LYP/6-31+G(d) level was eventually adopted as the level of geometry optimization, as this is the most cost-effective level that all the elusive species of interest can be obtained.

The optimized geometries of various species at the B3-LYP/6-31+G(d) level are summarized in Figures 1 and 2 for α- and β-Ala, respectively. With these optimized geometries, single-point calculations were carried out at the B3-LYP/6-311+G(3df,2p) level. The proton/alkali cation affinities at 0 K, ΔH_0, were obtained via eq 1

$$\Delta H_0 = [(E_{H^+/M^+} + E_L) - E_{H^+/M^+-L}] + [ZPE_L - ZPE_{H^+/M^+-L}] \times 0.9806 \quad (1)$$

where E_{H^+/M^+}, E_L, and E_{H^+/M^+-L} are the electronic energies of the proton/alkali cation, the α-/β-alanine ligand, and the protonated/alkali metal cationized complexes, respectively, calculated at the B3-LYP/6-311+G(3df,2p)//B3-LYP/6-31+G(d) level. The ZPE term denotes the zero-point energy of the various species calculated at the B3-LYP/6-31+G(d) level, scaled by 0.9806. Furthermore, to understand how the metal cation perturbs the stability of the covalent framework of the ligand, we calculated the deformation energy, E_{def}, at the B3-LYP/6-31+G(d) level of theory, where E_{def} is given by [17]

$$E_{def} = E(\text{ligand in the alkali metal cationized complex}) - E(\text{ligand in the uncomplexed form}) \quad (2)$$

Results and Discussion

Free α- and β-Alanine. The optimized geometries of free α- and β-Ala are displayed in Figures 1a and 2a, respectively. Here, we would like to highlight the differences between the most stable conformer of free α- and β-Ala. First, for α-Ala, a pair of intramolecular hydrogen bonds exists between the -NH_2 group and O=C sites, with quite similar interaction distances (refer to species **NU**, Figure 1a). For the **NU** form of β-Ala, one of the amino hydrogens is substantially further away (by over 1 Å) from the O=C site (Figure 2a). Given this rather long NH···O=C distance (3.67 Å), it is not clear whether one or two intramolecular hydrogen bonds exist in β-Ala. To answer this question, we carried out Atoms-In-Molecules (AIM)

TABLE 1: Electronic Energies (*E*, in Hartrees), Binding Affinities (ΔH_0 at 0 K in kJ mol^{-1}), Relative Affinities ($\Delta(\Delta H_0)$ in kJ mol^{-1}), and Deformation Energies (E_{def} in kJ mol^{-1}) of Free α- and *β*-Alanine and Its Protonated and Alkali Metal Cationized Complexes

	α-Ala				*β*-Ala			
species	E^a	$\Delta H_0{}^b$	$\Delta(\Delta H_0)^c$	$E_{def}{}^d$	E^a	$\Delta H_0{}^b$	$\Delta(\Delta H_0)^c$	$E_{def}{}^d$
				Free				
NU	−323.77075				−323.76909		0	
ZW					−323.69641		191	
				Protonated				
H$^+$(N)	−324.11265	898	0		−324.12159	925	0	
H$^+$(OC)	−324.07552	800	98		−324.07585	805	120	
H$^+$(OH)	−324.06318	768	130		−324.06565	779	146	
				Alkali metal cationized				
Li$^+$−CS1	−331.15105	250	0	35	−331.15652	269	0	34
Li$^+$−CS2	−331.13781	216	34	13	−331.14626	242	27	11
Li$^+$−ZW1	−331.14490	234	16	86	−331.14978	252	17	82
Li$^+$−ZW1′					−331.13099	202	67	199
Na$^+$−CS1	−485.92456	174	0	26	−485.92704	185	0	29
Na$^+$−CS2	−485.92077	164	10	8	−485.92769	187	−2	10
Na$^+$−ZW1	−485.92218	168	6	77	−485.92605	182	3	70
Na$^+$−ZW1′					−485.90397	124	61	191
K$^+$−CS1	−923.57620	117	0	25	−923.57805	126	0	24
K$^+$−CS2	−923.57853	123	−6	5	−923.58324	139	−13	2
K$^+$−ZW1	−923.57543	115	2	72	−923.57926	129	−3	62
K$^+$−ZW1′					−923.55371	62	64	188

[a] Calculated at the B3-LYP/6-311+G(3df,2p)//B3-LYP/6-31+G(d) level, with zero-point vibrational energy (ZPE) corrected at the B3-LYP/6-31+G(d) level. [b] Binding affinity at 0 K. [c] Relative binding affinity calculated with respect to the **NU** form (for free ligand); the **H$^+$(N)** form (for protonated system); and **CS1** form (for alkali metal cationized system). [d] Deformation energy is obtained at the B3-LYP/6-31+G(d) level of theory. This quantity is conceptually identical to the DIS term in eq 6. The numerical difference between E_{def} (in this table) and DIS (in Table 2) arises mainly from the difference in the level of theory employed.

analysis[18] and found no bond critical point (BCP) associated with this long NH···O═C distance. Thus, it suggests that only one set of intramolecular hydrogen bonds, as opposed to two sets in α-Ala, is present in the most stable form of *β*-Ala.

Second, it is well-known that, in the absence of solvent, the zwitterionic form of α-Ala is not stable in the gas phase: geometry optimization from the dipolar zwitterionic species would spontaneously yield the neutral form (**NU**) in which the amino proton is transferred to the carboxylate group.[19] With the methylene (−CH_2− group) at the *β*-position, extra conformation flexibility is created in *β*-Ala in which the <C−C−C−N torsional angle can be ∼0° (cis) or ∼180° (trans). While a proton shift is still spontaneous for *β*-Ala in the cis conformation, adopting the trans conformation allows sufficient separation between the two polar ends of the amino acid to deter a spontaneous proton shift. As a result, we found a zwitterionic form of *β*-Ala (species **ZW**, Figure 2a), in which the carboxylate carbon and the ammonium nitrogen is separated by ∼4.0 Å. However, as compared to the typical C−C (∼1.53 Å) and C−N (∼1.46 Å) bonds,[20] these two bonds are appreciably longer (∼0.08 Å) in the **ZW** form, reflecting the intrinsic instability of such species in the gas phase (191 kJ mol^{-1} less stable than the **NU** form, Table 1).

Protonated α- and *β*-Alanine. Three sites of protonation are available in both α- and *β*-Ala: the amino nitrogen, the carbonyl oxygen, and the hydroxyl oxygen, leading to the formation **H$^+$(N)**, **H$^+$(OC)**, and **H$^+$(OH)** protonated forms, respectively. The optimized structures for these various forms are shown in Figures 1b and 2b, respectively, for α- and *β*-Ala.

For α-Ala, it has been suggested that the most favorable site of protonation is the amino nitrogen.[13] The experimental proton affinity of 902 kJ mol^{-1} is in good agreement with what we estimated here for **H$^+$(N)** (898 kJ mol^{-1}, Table 1). We found that, for *β*-Ala, the most favorable site of protonation remains to be the amino nitrogen (Table 1). The experimental proton affinity of *β*-Ala determined recently by Hahn et al.[11] at 928 kJ mol^{-1} is also in very good agreement with our theoretical estimate of 925 kJ mol^{-1} (Table 1) for **H$^+$(N)**.

Interestingly, as compared to the other sites, protonation at the amino nitrogen is more favored in *β*-Ala than in α-Ala. We attribute this to the difference in the hydrogen bonding pattern between the two protonated amino acids. For protonated α-Ala, the intramolecular NH···O═C hydrogen bond leads to the formation of a five-membered ring motif with a hydrogen bonding distance of ∼2.0 Å. However, because of the additional methylene spacer in *β*-Ala, the hydrogen bond becomes part of a six-membered ring motif in **H$^+$(N)**, with a much shorter NH···O═C distance of ∼1.8 Å. This shorter (hence more stabilizing) intramolecular hydrogen bond further favors the formation of the protonated **H$^+$(N)** over **H$^+$(OC)** form in *β*-Ala than in α-Ala by 22 kJ mol^{-1}.

Alkali Metal Cationized α- and *β*-Alanine. The optimized geometries for the alkali metal cationized α- and *β*-alanine complexes are displayed in Figures 1c and 2c, respectively. In the following discussion, we shall use notations such as **CS1** to denote collectively the $Li^+/Na^+/K^+$-ligand complexes of a specific cation binding mode, while notations such as **Li$^+$−CS1** are used for the lithiated complex adopting the **CS1** mode of binding.

Previous theoretical studies suggested that alkali cations ($Li^+/Na^+/K^+$) are not capable of interacting simultaneously with all the basic sites present in α-amino acids, with the buildup of strain in the ligand cited to be the underlying cause.[21] With a more flexible backbone in *β*-Ala, we again explore the possibility of a tridentate metal cation binding mode, in which the M^+ will interact simultaneously with -NH_2, O═C, and -OH sites. However, as in the case of α-Ala, such mode of binding is found to be also unstable in *β*-Ala.

The general binding characteristics of M^+-*β*-Ala is similar to the corresponding mode in M^+-α-Ala, with the distances

between the alkali cation and the binding site(s) in β-alanine complexes being slightly shorter (on average 0.03 Å). One notable exception is the **Li$^+$−CS2** complex: whereas Li^+ binds bidentately to both O═C and -OH in α-Ala (Li^+···O distance 1.89 and 2.21 Å, respectively), a monodentate complex is formed in the case of β-Ala, with the Li^+···O═C bonding distance (1.77 Å) substantially shorter than the Li^+···OH distance (3.27 Å).

While the absolute M^+ affinity is enhanced from α- to β-Ala, the relative stabilities of different modes of binding show some interesting differences. In the case of α-Ala, it has been found previously[14] that the most stable mode of Li^+/Na^+ binding is bidentate, with the cation binding to the -NH_2 and O═C sites (**CS1**, Figure 1c) in a five-membered ring motif. For the larger K^+, the cation prefers to bind to the O═C and -OH sites (**CS2**, Figure 1c), forming a four-membered ring. In β-Ala (Figure 2c), while the **CS2** mode of binding is still a four-membered ring, the **CS1** mode is now a larger six-membered ring motif. Interestingly, our calculations suggest that while the **CS1** mode remains to be the most favored binding mode for the smallest Li^+, the **CS2** mode is now the preferred mode for Na^+/K^+. For the Na^+-β-Ala complex, the stability of the **Na$^+$−CS1** and **Na$^+$−CS2** complexes is quite comparable (2 kJ mol^{-1}, in favor of the latter). Given such a small difference, we further explored the effect of basis-set-superposition-error (BSSE) and electron correlation (at MP2(full)/6-311+G(3df,2p) level) on the relative stability of the two species. These additional calculations also support the finding that the most stable binding mode of the Na^+ bound complexes could be different in α- and β-Ala.

Hoyau et al. discussed the preference of **CS1** (M^+ binds to O═C and -NH_2) over **CS2** (M^+ binds to O═C and -OH) in M^+-α-Ala in terms of the destabilization of the five-membered ring moiety relative to other modes of binding.[21] We have suggested that as the difference in deformation energy, E_{def}, between the two modes is virtually independent of cationic size from Li^+ to Na^+ to K^+, the relative destabilization of the **CS1** mode for K^+ may not be caused by strains arising from binding to larger cations.[22] The case of β-Ala further supports this view. Not only does the difference in deformation energy between the two binding modes in M^+-β-Ala show little variation (23, 19, and 22 kJ mol^{-1} for $M^+ = Li^+$, Na^+, and K^+, respectively), they are almost identical to what is found for M^+-α-Ala (22, 18, and 20 kJ mol^{-1} for $M^+ = Li^+$, Na^+, and K^+, respectively). In other words, the preference of **CS1** versus **CS2** mode, as a function of cationic size, is not likely to be related to the ring-size/strain effect of the **CS1** mode (M^+ binding to both -NH_2 and O═C) but more likely to arise from the preference for nitrogen over oxygen for the larger alkali cation.[22]

The relative stabilities of the charge-solvated versus zwitterionic complexes of α-amino acids have been the subject of several publications.[22−24] The formation of zwitterionic structures is more favored by a greater proton affinity (PA) or basicity of the ligand, and with the increase of PA from α- to β-Ala (by ∼26 kJ mol^{-1}),[11] one may expect the relative stability of the zwitterionic mode to be enhanced. This indeed is observed for Na^+ and K^+ (Table 1): as compared to the **CS1** mode, the relative stability of the **ZW1** mode is enhanced by 3 and 5 kJ mol^{-1}, respectively, from α- to β-Ala. Despite this, as the relative stability of **CS2** mode over the **CS1** mode has increased even more by 12 and 7 kJ mol^{-1} for Na^+ and K^+, respectively, the most stable M^+ binding mode for β-Ala remains to be the charge-solvated form. Interestingly, for the smallest alkali cation, Li^+, the relative stability of the zwitterionic mode (**ZW1** vs **CS1**) is decreased marginally (by 1 kJ mol^{-1}) from α- to β-Ala. However, the origin of this rather unexpected trend is not clear.

TABLE 2: Natural Energy Decomposition Analysis (NEDA)[a] at the HF/6-31+G(d,p) Level, for the Various Lithiated and Potassiated Amino Acid Complexes[b]

species	CT	ES	POL	EX	DEF (M^+)	DEF (L)	ΔE	DIS[c]	ΔH_0[d]
				α-Ala					
Li$^+$−CS1	85	286	170	16	79	183	296	39	256
Li$^+$−CS2	51	216	127	10	45	121	238	37	201
Li$^+$−ZW1	68	337	146	15	65	146	354	132	222
K$^+$−CS1	15	162	140	20	64	130	143	28	116
K$^+$−CS2	16	146	103	15	44	101	134	25	109
K$^+$−ZW1	18	233	129	21	65	128	208	118	90
				β-Ala					
Li$^+$−CS1	102	308	187	18	92	208	316	37	279
Li$^+$−CS2	39	260	151	12	71	123	268	41	227
Li$^+$−ZW1	71	358	149	16	69	153	372	130	242
Li$^+$−ZW1′	76	431	145	17	74	157	438	236	201
K$^+$−CS1	19	174	153	22	73	142	152	26	126
K$^+$−CS2	16	166	111	16	48	110	151	29	122
K$^+$−ZW1	18	239	133	21	67	134	211	111	101
K$^+$−ZW1′	21	313	142	25	79	147	274	224	50

[a] The exact definition of the various components of the interaction energy, ΔE, can be found in ref 25. In brief, CT = charge transfer, ES = electrostatic, POL = polarization, EX = exchange, DEF = electronic deformation, and DIS = geometry deformation. [b] All energies are in units of kJ mol^{-1}. [c] The DIS term is conceptually identical to the E_{def} term in eq 2. The numerical difference between DIS (in this table) and E_{def} (in Table 1) arises solely from the level of theory from which the quantity is obtained. [d] The binding affinity at 0 K, ΔH_0, is given by the sum of the interaction energy (ΔE) and geometry deformation energy (DIS), eq 6. The numerical difference between the ΔH_0 term in Tables 1 and 2 is mainly due to the different level of theory employed but is also due to BSSE and zero-point vibrational energies. The value in Table 2 has been corrected with BSSE but not zero-point energies.

Furthermore, because of the increase in flexibility of its backbone, the formation of a zwitterionic conformer with ∼180° <C−C−C−N torsional angle becomes possible for β-Ala. It is interesting to compare this species, denoted as **ZW1′** (Figure 2c), with the free zwitterionic ligand **ZW** (Figure 2a). In the absence of the metal cation, the covalent C−C bond is noticeably long (∼1.62 Å, species **ZW** in Figure 2a). This bond is shortened by at least 0.08 Å in species **ZW1′** (Figure 2c), demonstrating clearly the effect of metal cation complexation on the geometry of a dipolar ligand.

In addition, comparing the relative stability of **ZW1′** with **ZW1**, the **ZW1** mode is favored for a larger cation. This increase in relative stability with increasing ionic size can be attributed to the stronger intramolecular electrostatic stabilization force present: for the **ZW1** mode of M^+-β-Ala, the NH_3^+···$^-$OCO bonding distance is shortened from 1.65 to 1.57 to 1.49 Å for $M^+ = Li^+$, Na^+, and K^+, respectively.

Natural Energy Decomposition Analysis on Lithiated and Potassiated α-/β-Alanine. Previously, Natural Energy Decomposition Analysis (NEDA) has been applied to study the origin of cation dependence of the relative stability of charge-solvated versus zwitterionic forms in alkaline earth cation−glycine complexes.[24] Here, we apply a similar analysis to study the lithiated and potassiated α/β-alanine complexes to understand the effects of ligand, cation size, and mode of binding on the interaction.

The different terms obtainable from NEDA analysis are summarized in Table 2. Under such a scheme, the total interaction energy, ΔE, is partitioned into five terms:[25]

$$\Delta E = \mathrm{CT} + \mathrm{ES} + \mathrm{POL} + \mathrm{EX} - \mathrm{DEF}(M^+) - \mathrm{DEF}(\mathrm{L}) \quad (3)$$

Here, the covalency component is described by the charge-transfer (CT) term, while the electrostatic and induced electrostatic terms are denoted by ES and POL terms, respectively. The exchange term, arising from Pauli exclusion principle, is given by EX. The energy penalties arising from disturbing the electron cloud in the metal cation and the ligand are given by DEF(M^+) and DEF(L) terms, respectively. For ease of discussion, we regroup the terms in eq 3 into

$$\mathrm{ELE} = \mathrm{ES} + \mathrm{POL} + \mathrm{EX} \tag{4}$$

$$\mathrm{DEF} = \mathrm{DEF}(M^+) + \mathrm{DEF}(\mathrm{L}) \tag{5}$$

in which ELE represents the favorable attractive interaction between M^+ and ligand arising from electrostatic, polarization, and exchange effects, and DEF is the sum of electronic deformation of the two monomers, M^+ and ligand L. Thus, the overall binding affinity, ΔH, is given by

$$\Delta H = (\mathrm{ELE} + \mathrm{CT}) - (\mathrm{DEF} + \mathrm{DIS}) \tag{6}$$

Here, the total favorable interaction is given by the sum of the ELE and the charge-transfer (CT) terms, while the total unfavorable interaction is given by the sum of DEF and geometry deformation (DIS). It is clear that ΔH (given in eq 6) and ΔE (given in eq 3) differs in the geometry deformation term, DIS, which is in fact conceptually identical to E_{def} (given in eq 2). Two different notations (DIS and E_{def}) are used here for consistency with literature from different groups.[17,24,25]

Currently, the NEDA partition scheme is only implemented at the Hartree−Fock level. Without accounting for the effect of electron correlation, we note that the binding affinity, ΔH, obtained at the HF/6-31+G(d,p) level (Table 2) tends to be smaller by up to 28 kJ mol^{-1} when compared to that obtained at the B3-LYP/6-311+G(3df,2p) level (Table 1). Even though the HF/6-31+G(d,p) level of theory fails to reproduce the preference of $\mathbf{K^+}$−**CS2** over $\mathbf{K^+}$−**CS1**, the other trends on relative stabilities are generally reproduced. Therefore, we believe NEDA is still valuable in providing a semiquantitative description of the interaction between the alkali cation and α-/*β*-Ala.

The variations of the ELE and CT terms are displayed in Figure 3a, while that of the DEF and DIS terms are shown in Figure 3b. These figures clearly reveal that the overall attractive interaction (Figure 3a) overweighs the overall unfavorable interaction (Figure 3b), so that the binding of M^+ to α/*β*-alanine is favorable. Furthermore, the ELE component is much larger than the CT component, thus confirming that the interaction between an alkali cation and the ligands is largely electrostatic in nature.[14,21−26]

Ligand Effect. For the same cation and with the same binding mode, the ELE, CT, and DEF terms in general increase from α- to *β*-Ala. At the same time, because of the close resemblance of binding characteristics, the destabilization effect arising from geometry deformation, DIS, is rather constant. Thus, the general increase of alkali metal cation affinities from α- to *β*-Ala is mostly due to the enhancement of the attractive interaction, rather than the decrease in the destabilization factor.

Binding Mode Rffect. The slightly higher stability for the **CS2**/**ZW1** mode (over **CS1**) in K^+-*β*-Ala cannot be reproduced at the HF/6-31+G(d,p) level. We carried out similar analysis at the HF level with a larger basis set (6-311+G(3df,2p)) but found qualitatively the same result. Thus, it appears that electron correlation treatment is important, and detailed analysis of the nature of binding mode effect based on Hartree−Fock wave functions may not be appropriate.

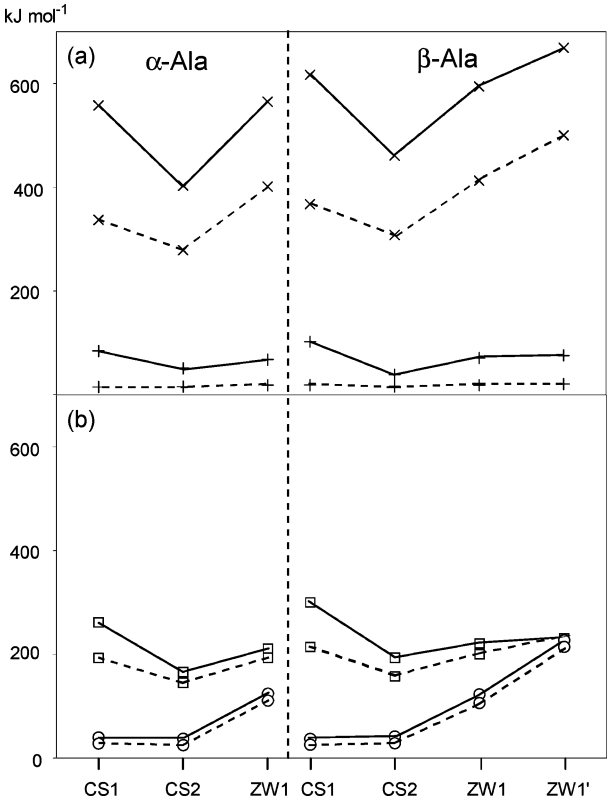

Figure 3. Variation of various components of the binding affinity, based on NEDA analysis of the HF/6-31+G(d,p) wave function, as a function of binding modes for (a) the attractive interactions (x = ELE, + = CT) and (b) unfavorable interactions (□ = DEF, ○ = DIS). The data points for Li^+ and K^+ complexes are connected by solid and dotted lines, respectively.

However, the NEDA clearly indicates that the interaction energy, ΔE, for the zwitterionic modes (**ZW1** and **ZW1′**) is larger than that of the charge-solvated modes (**CS1** and **CS2**), but at the same time, these binding modes are also subjected to a larger geometry deformation effect (DIS). As a result, the Li^+ and K^+ binding affinities of the zwitterionic modes, ΔH, are often smaller than the charge-solvated modes. It also appears that the dominant component in stabilizing the zwitterionic mode is the static electrostatic interaction term (ES), as the induced interaction term (POL) is not necessarily larger in these zwitterionic modes.

One interesting trend is noted when one compares the magnitude of the various components for the $\mathbf{Li^+}$−**CS2** mode of α- and *β*-Ala. For the $\mathbf{K^+}$−**CS2**, $\mathbf{Li^+}$/$\mathbf{K^+}$−**CS1**, and $\mathbf{Li^+}$/$\mathbf{K^+}$−**ZW1** modes, the CT, ES, and POL terms all increase slightly from α- to *β*-Ala. For the $\mathbf{Li^+}$−**CS2** mode, the CT component decreases from α- to *β*-Ala, while the ES and POL components increase quite significantly. We attribute this to the change in cation binding in $\mathbf{Li^+}$−**CS2**: from monodentate in *β*-Ala to bidentate in α-Ala. The physical origin of this is not clear, but it has also been reported in the case of $Li(H_2O)_n^+$ (where $n = 1-4$), the CT component increases with increasing number of water molecules coordinated to the Li^+.[25]

Ionic Size Effect. For the same mode of binding to α-/*β*-Ala, the binding affinity decreases from Li^+ to K^+. This has largely been attributed to the decrease in attractive interactions with increasing ionic radii.[14,21−26] Here, NEDA provides further insight into the origin of this decrease in binding affinity. With the increase in ionic radii, not only does the ELE component decrease, but the CT component also decreases. In percentage terms, the decrease in the covalent CT component is in fact

more pronounced. Typically, when the ELE component is decreased by 20−30% from Li^+ to K^+, the CT component decreases by 60−80%, so that the electrostatic component becomes even more dominant in the overall stabilization of the larger K^+ complexes.

Last, we would like to compare our result for Li^+-α-Ala (Table 2) with that of Be^{2+}-glycine published previously.[24] It should be noted here that the ligands in the two studies are different. However, given the similarity between glycine (Gly) and Ala, we believe that such a comparison is meaningful in understanding the similarity/difference in mono versus dication binding to the aliphatic α-amino acids. At the HF/6-31+G(d,p) level, for the same mode of binding, the cation affinity has increased by about 5−6-fold from Li^+ to Be^{2+}. While both ELE and CT components are increased from Li^+ to Be^{2+}, the increase in the CT component is more obvious. This suggests that, even though the electrostatic component remains to be the dominant stabilizing term in the interaction between Li^+/Be^{2+} and amino acid, the charge-transfer effect has become more important in the dication. This arises from the closer interaction distance between the dication and the ligand-binding site, which allows better orbital overlap, thus increasing the CT component. Another factor to be noted is the geometry deformation, as indicated by the DIS term in eq 6. Interestingly, while the DIS term of the charge-solvated **CS1** mode increases from Li^+ to Be^{2+}, the same term has decreased for the zwitterionic **ZW1** mode. This suggests that for alkali (monocation) and alkaline earth cation (dication) in the same row of the periodic table, the dication would favor the formation of the zwitterionic complex via the combined effects of the stronger attraction (from the CT component) and the diminished geometry deformation of the ligand.

Conclusions

Density functional theory calculations have been used to model the α/β-alanine and their cationic (proton and alkali cation) complexes. Despite being inert, the presence of a methylene group ($-CH_2-$) at the β position leads to some interesting physicochemical changes from α- to β-Ala:

(1) the preferred hydrogen-bonding pattern in the free amino acids is altered so that in β-Ala, only one set of intramolecular hydrogen bonds is present.

(2) The enhanced conformation flexibility in β-Ala indirectly leads to the formation of a stable zwitterionic form in the gas phase, even though this zwitterionic form is not the global minima in this system.

(3) Proton affinity is enhanced in β-Ala, with the protonation at the amino nitrogen even more preferred over the other basic sites.

(4) Alkali cation affinity is also enhanced in β-Ala. While the most preferred mode of binding for Li^+ and K^+ is identical to what is found in α-Ala, the preferred mode of Na^+ has been changed from O═C, $-NH_2$ in α-Ala to O═C, -OH in β-Ala.

Finally, the interaction between the alkali cation and the amino acids is analyzed using Natural Energy Decomposition Analysis to gain further insight into the effects of ligand, cation size, and the mode of binding on alkali metal chelation. The binding interaction is predominantly electrostatic in nature, as opposed to charge transfer, with the electrostatic term playing a more important role in the zwitterionic modes of binding. By comparing a previous report on dication−amino acid complexes, it appears that the dication would favor the formation of zwitterionic complex via the combined effects of the stronger attraction (with contribution predominantly from the charge-transfer component) and diminished geometry deformation of the ligand.

Acknowledgment. The generous allocation of supercomputer time and the award of a postgraduate studentship from the Institute of High Performance Computing to S.A. are gratefully acknowledged. The funding supports of the Hong Kong Polytechnic University (Area of Strategic Development Fund Project No. A024 to C.W.T.) and the Research Grant Council of Hong Kong (Area of Excellence Project No. P-10/2001 and CERG Project No. PolyU 5012/04P to C.W.T.) are gratefully acknowledged.

References and Notes

(1) Sewald, N. In *Bioorganic Chemistry: Highlights and New Aspects*; Diederichsen, U., Lindhorst, T. K., Westermann, B., Wessjohann, L. A., Eds.; Wiley: New York, 1999.

(2) Maar, T. E.; Lund, T. M.; Gegelashvili, G.; Hartmann-Petersen, R.; Moran, J.; Pasantes-Morales, H.; Berezin, V.; Bock, E.; Schousboe, A. *Amino Acids* **1988**, *15*, 77.

(3) Kyrikou, I.; Grdadolnik, S. G.; Tatari, M.; Poulos, C.; Mavromoustakos, T. *J. Pharm. Biomed. Anal.* **2003**, *31*, 713.

(4) (a) Hipkiss, A. R.; Brownson, C. *Cell. Mol. Life Sci.* **2000**, *57*, 747. (b) Baran, E. J. *Biochemistry (Mosc.)* **2000**, *65*, 789. (c) Hipkiss, A. R.; Brownson, C.; Carrier, M. J. *Mech. Aging Dev.* **2001**, *122*, 1431. (d) Teufel, M.; Saudek, V.; Ledig, J.-P.; Bernhardt, A.; Boularand, S.; Carreau, A.; Cairns, N. J.; Carter, C.; Cowley, D. J.; Duverger, D.; Ganzhorn, A. J.; Guenet, C.; Heintzelmann, B.; Laucher, V.; Sauvage, C.; Smirnova, T. *J. Biol. Chem.* **2003**, *278*, 6521.

(5) Fujii, T.; Takaoka, M.; Muraoka, T.; Kurata, H.; Tsuruoka, N.; Ono, H.; Kiso, Y.; Tanaka, T.; Matsumura, Y. *Eur. J. Pharmacol.* **2003**, *474*, 261.

(6) Hook, D. F.; Gessier, F.; Noti, C.; Kast, P.; Seebach, D. *ChemBioChem* **2004**, *5*, 691 and references therein.

(7) (a) Gademann, K.; Ernst, M.; Hoyer, D.; Seebach, D. *Angew. Chem., Int. Ed.* **1999**, *38*, 1223. (b) Werder, M.; Hauser, H.; Abele, S.; Seebach, D. *Helv. Chim. Acta* **1999**, *82*, 1774. (c) Porter, E. A.; Wang, X. F.; Lee, H. S.; Weisblum, B.; Gellman, S. H. *Nature* **2000**, *404*, 565. (d) Raguse, T. L.; Porter, E. A.; Weisblum, B.; Gellman, S. H. *J. Am. Chem. Soc.* **2002**, *124*, 12774. (e) Steer, D. L.; Lew, R. A.; Perlmutter, P.; Smith, I.; Aguilar, M.-I. *Lett. Pept. Sci.* **2002**, *8*, 241.

(8) Kaim, W.; Schwederski, B. *Bioinorganic Chemistry: Inorganic Elements in the Chemistry of Life: An Introduction and Guide*; Wiley: Chichester, 1994.

(9) (a) Wu, Z.; Fenselau, C. *Tetrahedron* **1993**, *49*, 9197. (b) Carr, S. R.; Cassady, C. J. *J. Am. Soc. Mass Spectrom.* **1996**, *7*, 1203. (c) Harrison, A. G. *Mass Spectrom. Rev.* **1997**, *16*, 201. (d) Maksic, Z. B.; Kovacevic, B. *Chem. Phys. Lett.* **1999**, *307*, 497. (e) Pepe, C.; Rochut, S.; Paumard, J.-P.; Tabet, J.-C. *Rapid Commun. Mass Spectrom.* **2004**, *18*, 307.

(10) (a) Andersen, U. N.; Bojesen, G. *J. Chem. Soc., Perkin Trans. 2* **1997**, 323. (b) Cerda, B. A.; Hoyau, S.; Ohanessian, G.; Wesdemiotis, C. *J. Am. Chem. Soc.* **1998**, *120*, 2437. (c) Gapeev, A.; Dunbar, R. C. *J. Am. Chem. Soc.* **2001**, *123*, 8360. (d) Moision, R. M.; Armentrout, P. B. *J. Phys. Chem. A* **2002**, *106*, 10350. (e) Feng, W. Y.; Gronert, S.; Lebrilla, C. B. *J. Phys. Chem. A* **2003**, *107*, 405. (f) Kish, M. M.; Ohanessian, G.; Wesdemiotis, C. *Int. J. Mass Spectrom.* **2003**, *227*, 509. (g) Gapeev, A.; Dunbar, R. C. *Int. J. Mass Spectrom.* **2003**, *228*, 825.

(11) Hahn, I.-S.; Wesdemiotis, C. *Int. J. Mass Spectrom.* **2003**, *222*, 465.

(12) Császár, A. G. *J. Phys. Chem.* **1996**, *100*, 3541.

(13) Topol, I. A.; Burt, S. K.; Toscano, M.; Russo, N. *J. Mol. Struct. (THEOCHEM)* **1998**, *430*, 41.

(14) Marino, T.; Russo, N.; Toscano, M. *Inorg. Chem.* **2001**, *40*, 6439.

(15) *SYBYL 6.7*; Tripos, Inc.: St. Louis, MO.

(16) Frisch, M. J.; Trucks, G. W.; Schlegel, H. B.; Scuseria, G. E.; Robb, M. A.; Cheeseman, J. R.; Zakrzewski, V. J.; Montgomery, J. A., Jr.; Stratmann, R. E.; Burant, J. C.; Dapprich, S.; Millam, J. M.; Daniels, A. D.; Kudin, K. N.; Strain, M. C.; Farkas, O.; Tomasi, J.; Barone, V.; Cossi, M.; Cammi, R.; Mennucci, B.; Pomelli, C.; Adamo, C.; Clifford, S.; Ochterski, J.; Petersson, G. A.; Ayala, P. Y.; Cui, Q.; Morokuma, K.; Malick, D. K.; Rabuck, A. D.; Raghavachari, K.; Foresman, J. B.; Cioslowski, J.; Ortiz, J. V.; Baboul, A. G.; Stefanov, B. B.; Liu, G.; Liashenko, A.; Piskorz, P.; Komaromi, I.; Gomperts, R.; Martin, R. L.; Fox, D. J.; Keith, T.; Al-Laham, M. A.; Peng, C. Y.; Nanayakkara, A.; Gonzalez, C.; Challacombe,

M.; Gill, P. M. W.; Johnson, B.; Chen, W.; Wong, M. W.; Andres, J. L.; Gonzalez, C.; Head-Gordon, M.; Replogle, E. S.; Pople, J. A. *Gaussian 98, revision A11.3*; Gaussian, Inc.: Pittsburgh, PA, 2002.

(17) Wong, C. H. S.; Siu, F. M.; Ma, N. L.; Tsang, C. W. *J. Mol. Struct. (THEOCHEM)* **2002**, *588*, 9.

(18) Bader, R. F. W. *Atoms in Molecules. A Quantum Theory*; Clarendon: Oxford, 1990.

(19) Nobrega, G. F.; Sambrano, J. R.; de Souza, A. R.; Queralt, J. J.; Longo, E. *J. Mol. Struct. (THEOCHEM)* **2001**, *544*, 151.

(20) *CRC HandBook of Chemistry and Physics*; Lide, D. R., Ed.; CRC Press: Boca Raton, FL, 2002−2003; 83rd ed.

(21) Hoyau, S.; Ohanessian, G. *Chem.−Eur. J.* **1998**, *4*, 1561.

(22) Siu, F. M.; Ma, N. L.; Tsang, C. W. *Chem.−Eur. J.* **2004**, *10*, 1966.

(23) Wyttenbach, T.; Witt, M.; Bowers, M. T. *Int. J. Mass Spectrom.* **1999**, *182/183*, 243. (b) Jockusch, R. A.; Price, W. D.; Williams, E. R. *J. Phys. Chem. A* **1999**, *103*, 9266. (c) Cerda, B. A.; Wesdemiotis, C. *Analyst* **2000**, *125*, 657. (d) Wyttenbach, T.; Witt, M.; Bowers, M. T. *J. Am. Chem. Soc.* **2000**, *122*, 3458. (e) Siu, F. M.; Ma, N. L.; Tsang, C. W. *J. Am. Chem. Soc.* **2001**, *123*, 3397.

(24) Strittmatter, E. F.; Lemoff, A. S.; Williams, E. R. *J. Phys. Chem. A* **2000**, *104*, 9793.

(25) Glendening, E. D. *J. Am. Chem. Soc.* **1996**, *118*, 2473.

(26) (a) Rodgers, M. T.; Armentrout, P. B. *Mass Spectrom. Rev.* **2000**, *19*, 215. (b) Talley, J. M.; Cerda, B. A.; Ohanessian, G.; Wesdemiotis, C. *Chem.−Eur. J.* **2002**, *8*, 1377. (c) Lau, J. K. C.; Wong, C. H. S.; Ng, P. S.; Siu, F. M.; Ma, N. L.; Tsang, C. W. *Chem.−Eur. J.* **2003**, *9*, 3383.